/
Article / Book Information

Title	Band gap engineering based on Mg_x_Zn_1-x_O and Cd_y_Zn_1-y_O ternary alloy films
Authors	T. Makino,Y. Segawa,M. Kawasaki,A. Ohtomo,R. Shiroki,K. Tamura,T. Yasuda,H. Koinuma
Citation	Applied Physics Letters, Vol. 78, No. 9,
Pub. date	2001, 2
URL	http://scitation.aip.org/content/aip/journal/apl
Copyright	Copyright (c) 2001 American Institute of Physics

Band gap engineering based on $Mg_xZn_{1-x}O$ and $Cd_yZn_{1-y}O$ ternary alloy films

T. Makino[a)] and Y. Segawa
Photodynamics Research Center, RIKEN (Institute of Physical and Chemical Research), Sendai 980-0845, Japan

M. Kawasaki, A. Ohtomo,[b)] R. Shiroki, and K. Tamura
Department of Innovative and Engineered Materials, Tokyo Institute of Technology, Yokohama 226-8502, Japan

T. Yasuda[c)]
School of Science and Engineering, Ishinomaki Senshu University, Ishinomaki 986-8580, Japan

H. Koinuma[d)]
Materials and Structures Laboratory, Tokyo Institute of Technology, Yokohama 226-8503, Japan

We describe the structural and optical properties of II–VI oxide alloys, $Mg_xZn_{1-x}O$ and $Cd_yZn_{1-y}O$, grown by pulsed-laser deposition. Single-phase alloyed films of (Mg,Zn)O and (Cd,Zn)O with c-axis orientations were epitaxially grown on sapphire (0001) substrates. The maximum magnesium and cadmium concentrations ($x=0.33$ and $y=0.07$, respectively) were significantly larger than the thermodynamic solubility limits. The band gap energies systematically changed from 3.0 ($y=0.07$) to 4.0 eV ($x=0.33$) at room temperature. The photoluminescence peak energy deduced at 4.2 K could be tuned from 3.19 to 3.87 eV by using $Cd_{0.07}Zn_{0.93}O$ and $Mg_{0.33}Zn_{0.67}O$ at both ends, respectively. The lattice constants of the a axis were monotonically increasing functions of the concentrations of both alloys. The exciton–phonon coupling strength was determined in $Cd_{0.01}Zn_{0.99}O$ grown on a lattice-matched $ScAlMgO_4$ substrate. © *2001 American Institute of Physics.* [DOI: 10.1063/1.1350632]

Much interest has recently been shown in ZnO as a promising candidate for ultraviolet optical applications such as light-emitting diodes or laser diodes. Its large exciton binding energy of 59 meV (Ref. 1) has enabled observation of laser action and/or stimulated emission of exciton is origins at temperatures well above room temperature (RT) in ZnO thin films[2–4] and in ZnO/(Mg,Zn)O superlattices (SLs).[5] Such observations indicate that an exciton-related recombination process can be utilized in optoelectronic devices based on ZnO. A lower pumping threshold can be expected, in principle, if exciton-related recombination is used, rather than recombination of an electron-hole plasma, which is the dominant mechanism of laser action in (In,Ga)N devices. Fabrication and characterization of alloys such as (Mg,Zn)O or (Cd,Zn)O are important from the viewpoint of band gap engineering as well as of a *p-n* junction. A $Mg_xZn_{1-x}O$ alloy has been found to be a suitable material for the barrier layers of ZnO/(Mg,Zn)O SLs due to its wider band gap.[6,7] On the other hand, a (Cd,Zn)O mixed crystal is expected to expand the wavelength tunability by virtue of its narrower band gap. Because the ionic radius of Cd^{2+} (0.74 Å) is close to that of Zn^{2+} (0.60 Å), the wurtzite (WZ) phase, which is a stable phase of ZnO, is expected to be conserved when a rock-salt (RS)-structured CdO is alloyed. There have been, however, few experimental studies on the properties of this alloyed epitaxial film.[8,9] In this letter, we describe the structural and

optical properties of $Cd_yZn_{1-y}O$ and $Mg_xZn_{1-x}O$ alloys. Since laser actions in ZnO-related materials are of excitonic origin, precise determination of the excitonic parameters is important.

Alloyed $Cd_yZn_{1-y}O$ films were grown on sapphire (0001) and $ScAlMgO_4$ (0001) substrates[10–12] by pulsed-laser deposition (PLD) in an ultrahigh vacuum chamber. The targets were ablated by excimer laser pulses. The films ($\sim$200 nm in thickness) were deposited at 400 °C in 5×10^{-5} Torr of pure oxygen. The cadmium content in the $Cd_yZn_{1-y}O$ films was determined by electron probe microanalyses as well as by induction coupling plasma optical emission spectroscopy. The cadmium contents in the alloyed films were slightly lower than those in the targets, due to the difference between the vapor pressures of Cd and Zn. The surface morphology of the films was examined using contact-mode atomic force microscopy. The crystal structure of the films was analyzed using a high-resolution x-ray diffraction (XRD) apparatus. Optical properties were characterized by absorption spectroscopy. A He–Cd laser (325 nm) was used for the photoluminescence (PL) measurements.

The XRD study revealed that all of the films had c-axis orientation and WZ phase without any impurity phase (e.g., RS phase). The maximum Cd content was $y=0.07$ which is significantly larger than the thermodynamic solubility limit ($y=0.02$). Figure 1(a) shows the cadmium content dependence of the full widths at half maximum (FWHMs) of the ZnO(0002) peaks in x-ray curves obtained by ω and $\omega-2\theta$ scans. The measured film was grown on sapphire substrates. As the cadmium content increased, both of the FWHMs increased. Considerable degradation, presumably due to large
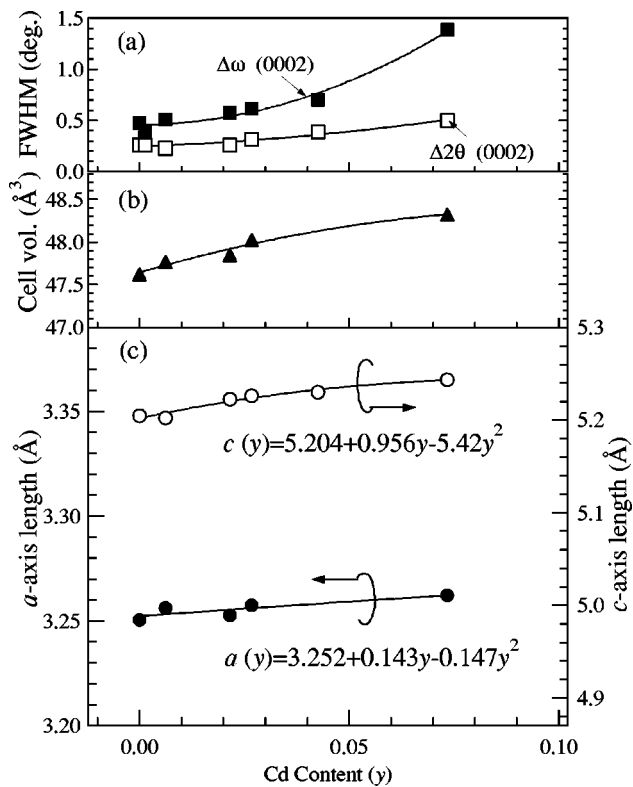
FIG. 1. Cadmium content dependence of (a) FWHM values of the (0002) peak in XRD ω and $\omega-2\theta$ scanned curves, (b) dependence of the cell volume, and (c) dependence of the a- and c-axis lattice lengths of the $Cd_yZn_{1-y}O$ films grown on sapphire substrates. The solid lines in (c) are fitted lines obtained by using $a=3.252+0.143y-0.147y^2$ and $c=5.204+0.956y-5.42y^2$.

FIG. 2. Concentration (y) dependence of absorption spectra of $Cd_yZn_{1-y}O$ epilayers obtained at room temperature. The curves, from right to left- correspond to those of the samples with $y=0$, 0.0013, 0.027, 0.043, and 0.073.

compositional fluctuation at $y\geqslant0.05$, was observed. The cell volume ($\sqrt{3}/2a^2c$) and a- and c-axis lengths determined by XRD are plotted as functions of Cd content in Figs. 1(b) and 1(c), respectively. The cell volume varied 1.5% at $y=0.07$ from that of pure ZnO, which is in a good agreement with the predicted value (1.6%) obtained by assuming that this difference is caused by the difference in the cation radii of Cd^{2+} and Zn^{2+}. Both a- and c-lattice constants were monotonically increasing functions of y and could be fitted by $a=3.252+0.143y-0.147y^2$ and $c=5.204+0.956y-5.42y^2$, respectively. The ratio of c/a was also a monotonically increasing function of y, in contrast to that in (Mg,Zn)O alloys. This could be explained by the magnitudes of electronegativity of the compounds, i.e., $\mathcal{F}_{Mg}>\mathcal{F}_{Zn}>\mathcal{F}_{Cd}$ ($\mathcal{F}$ denoting electron negativity). We tested the thermal stability of the $Cd_yZn_{1-y}O$ films. Annealing at a temperature of 700 °C improved the compositional homogeneity as well as the crystallinity, while annealing at 800 °C in air caused a considerable reduction in the Cd concentration due to its evaporation.

Figure 2 shows concentration (y) dependence of absorption spectra in as-grown films obtained at room temperature. The energy of the band gap (E_g) shifted downward when y increased. The spectrum of $Cd_{0.073}Zn_{0.927}O$ encompassed a broad shoulder on the lower energy side, indicating the formation of a cadmium-rich phase, the density of which is relatively low. Energies (E_g) are plotted in the inset of Fig. 2. We could fit the y dependence of the E_g values by a well-known equation in polynomial form,[13] and it was estimated as $E_g(y)=3.29-4.40y+5.93y^2$. Band gap narrowing

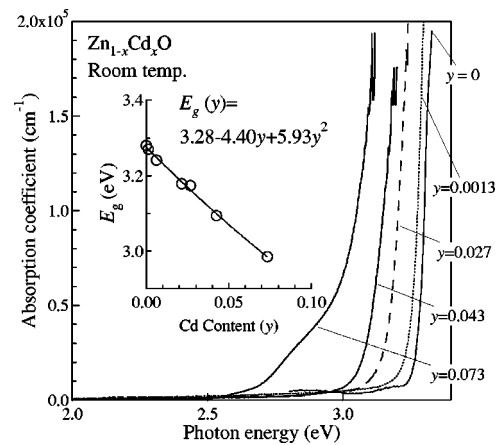down to 2.99 eV could be achieved by incorporating Cd^{2+} with $y=0.07$. PL spectra obtained at room temperature exhibited a single PL band, the peak energy of which approximately coincided with those in absorption spectra. The photoluminescence peak energy deduced at 4.2 K could be tuned from 3.19 to 3.87 eV by using $Cd_{0.07}Zn_{0.93}O$ and $Mg_{0.33}Zn_{0.67}O$, respectively.

Figure 3 shows the a-axis lengths as a function of room-temperature E_g values in $Cd_yZn_{1-y}O$ and $Mg_xZn_{1-x}O$ alloys. A (Cd,Zn)O/(Mg,Zn)O (CZM) SL, having a perfect (in-plane) lattice match and a maximum barrier height of 0.09 eV, can be obtained by choosing an appropriate combination of Cd and Mn concentrations,[8] because both a-axis lengths are monotonically increasing functions of concentrations of both alloys. This is one advantage compared to (In,Ga)N/(Al,Ga)N SLs. The same parametric plots in (In,Ga)N and (Al,Ga)N are shown by dashed curves. In the case of WZ, if the lattice constant of the well layer differs from that of the barrier layer, strain and a piezoelectric field exist
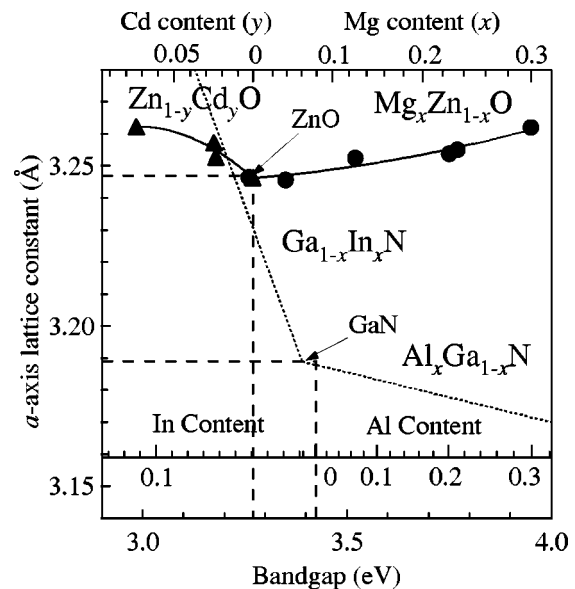

FIG. 3. Optical and structural properties of $Cd_yZn_{1-y}O$ and $Mg_xZn_{1-x}O$ alloy films mapped out in a plane of a-axis length and room-temperature band gap energy. The same curves for (In,Ga)N and (Al,Ga)N alloys are also shown. Alloy compositions are shown at the top axis.

Material	λ (meV)	$\hbar\bar{\omega}$ (meV)
ZnO[a]	66	22
CdZnO	66	22

[a]From Ref. 12.

pling strength. Table I shows λ and $\hbar\bar{\omega}$ of (Cd,Zn)O and ZnO. These two quantities of (Cd,Zn)O were similar to those of ZnO.[12,16]

In summary, II–VI semiconductor alloy $Cd_y Zn_{1-y}O$ films ($0 \leq y \leq 0.07$) were grown by PLD. The maximum Cd content determined in this study is significantly larger than the thermodynamic solubility limit ($y = 0.02$). The band gap could be tuned to the lower energy side by 0.3 eV at $y = 0.07$ in comparison with that of ZnO. Strain-free SL structures having a maximum barrier height of 0.9 eV can be fabricated by combining them with the wider-gap $Mg_x Zn_{1-x}O$. The enlarged solubility attained by nonequilibrium PLD growth and the perfectly lattice-matched heterojunction open new possibilities for an active layer in blue LEDs based on ZnO.
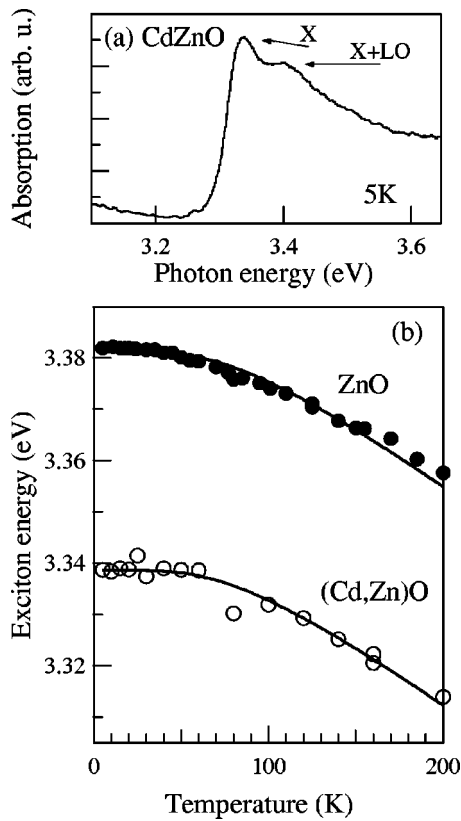
FIG. 4. (a) Absorption spectra in a $Cd_y Zn_{1-y}O$ ($y = 0.01$) epilayer grown on a lattice-matched $ScAlMgO_4$ substrate obtained at 5 K. (b) Temperature dependence of absorption peak energy in (Cd,Zn)O (open circles) and ZnO (closed circles). Solid curves are the fitted results obtained using Eq. (1).

inside the well layers. An internal electric field spatially separates the electrons and holes confined in well layers and, therefore, makes the excitonic properties complicated. The optical properties of almost perfectly lattice-matched CZM SLs have been reported elsewhere.[9]

Finally, we tried to deduce the exciton–phonon coupling strengths of (Cd,Zn)O thin films. We used a relatively thin (50 nm in thickness) epilayer grown on a lattice-matched (0.08%) $ScAlMgO_4$ substrate.[10–12] The use of this lattice-matched substrate improved the optical properties and suppressed undesirable broadening in the exciton resonance spectra.[12] An absorption spectrum obtained at 5 K in $Cd_y Zn_{1-y}O$ ($y = 0.01$) is shown in Fig. 4(a). Two peaks, labeled X and $X+LO$, can be seen. These were attributed to transitions to free exciton states (the A and B excitons overlap) and to exciton–phonon complex states,[14] respectively. The peak energies of the X band are plotted against temperature (5–200 K) in Fig. 4(b) for (Cd,Zn)O (open circles) and for ZnO (closed circles)[12] (weighted average of A- and B-exciton energies). A shift in the exciton energy as a function of temperature results essentially from a band gap shift. This is derived from both thermal expansion and exciton–phonon interaction. The temperature-induced shift can be reproduced by the Bose–Einstein approximation[15] using the effective phonon energy $\hbar\bar{\omega}$ and the variation of exciton energy with T (temperature) and is given by

$$E(T) = E(0) - \lambda / [\exp(\hbar\bar{\omega}/k_B T) - 1], \quad (1)$$

where $E(0)$ is exciton resonance energy at $T = 0$ K, and λ is a proportional coefficient related to the exciton–phonon cou-

[1] K. Hümmer, Phys. Status Solidi B **56**, 249 (1973).
[2] P. Yu, Z. K. Tang, G. K. L. Wong, M. Kawasaki, A. Ohtomo, H. Koinuma, and Y. Segawa, in *Proccedings of the 23rd International Conference on Physics of Semiconductors, Berlin*, edited by M. Scheffler and R. Zimmermann (World Scientific, Singapore, 1996), Vol. 2, p. 1453.
[3] P. Yu, Z. K. Tang, G. K. L. Wong, M. Kawasaki, A. Ohtomo, H. Koinuma, and Y. Segawa, Solid State Commun. **103**, 459 (1997).
[4] D. M. Bagnall, Y. F. Chen, Z. Zhu, T. Yao, S. Koyama, M. Y. Shen, and T. Goto, Appl. Phys. Lett. **70**, 2230 (1997).
[5] A. Ohtomo, K. Tamura, M. Kawasaki, T. Makino, Y. Segawa, Z. K. Tang, G. Wong, Y. Matsumoto, and H. Koinuma, Appl. Phys. Lett. **77**, 2204 (2000).
[6] A. Ohtomo, M. Kawasaki, T. Koida, K. Masubuchi, H. Koinuma, Y. Sakurai, Y. Yoshida, T. Yasuda, and Y. Segawa, Appl. Phys. Lett. **72**, 2466 (1998).
[7] A. Ohtomo, R. Shiroki, I. Ohkubo, H. Koinuma, and M. Kawasaki, Appl. Phys. Lett. **75**, 4088 (1999).
[8] M. Kawasaki, A. Ohtomo, R. Shiroki, I. Ohkubo, H. Kimura, G. Isoya, T. Yasuda, Y. Segawa, and H. Koinuma, *Extended Abstracts of the 1998 International Conference on Solid State Devices and Materials* (Business Center, Academic Society of Japan, Hiroshima, Japan, 1998), p. 356.
[9] T. Makino, N. T. Tuan, Y. Segawa, C. H. Chia, M. Kawasaki, A. Ohtomo, K. Tamura, and H. Koinuma, Appl. Phys. Lett. **77**, 1632 (2000).
[10] A. Ohtomo, K. Tamura, K. Saikusa, T. Takahashi, T. Makino, Y. Segawa, H. Koinuma, and M. Kawasaki, Appl. Phys. Lett. **75**, 2635 (1999).
[11] K. Tamura, A. Ohtomo, K. Saikusa, Y. Osaka, T. Makino, Y. Segawa, M. Sumiya, S. Fuke, H. Koinuma, and M. Kawasaki, J. Cryst. Growth **214/215**, 59 (2000).
[12] T. Makino, C. H. Chia, N. T. Tuan, Y. Segawa, M. Kawasaki, A. Ohtomo, K. Tamura, and H. Koinuma, Appl. Phys. Lett. **76**, 3549 (2000).
[13] J. V. Vechten and T. K. Bergstresser, Phys. Rev. B **1**, 3351 (1970).
[14] W.Y. Liang and A. D. Yoffe, Phys. Rev. Lett. **20**, 59 (1968).
[15] P. Lautenschlager, M. Garriga, S. Logotheitidis, and M. Cardona, Phys. Rev. B **35**, 9174 (1987).
[16] The deduced λ in Ref. 12, is not precise because the temperature range under examination was limited to 5–150 K. A more precise value, which can be obtained by expanding the temperature range, is shown in Table I.